The Trapping of Short-Lived Carbene Species with *tert*-Butyl Isocyanide to Form Infrared Active Adducts

A Senior Honors Thesis

Presented in Partial Fulfillment of the Requirements for graduation
with distinction in Chemistry in the undergraduate colleges
of The Ohio State University

by

George Joseph Holinga

The Ohio State University
June 2005

Project Advisor: Professor Matthew Platz, Department of Chemistry

ABSTRACT

A technique was developed for trapping infrared inactive carbenes with a standard reagent to produce infrared active adducts that can be directly observed using nanosecond time-resolved infrared spectroscopy. A complication of measuring the generation, presence, and reactivity of carbene species is that these transient species often have very short lifetimes ($\tau \leq$ 500 ns) and do not strongly absorb infrared radiation. While several standard methods such as laser-flash photolysis exist for measuring reaction kinetics of these transient structures using ultraviolet-visible wavelengths, currently a standard method for monitoring highly reactive carbene species at infrared wavelengths does not exist. The ability to directly observe such species with infrared wavelengths would be particularly helpful because vibrational spectra can be used to provide chemical structural information far beyond that of ultraviolet-visible (electronic) spectroscopy.

Nanosecond time-resolved infrared spectroscopy was conducted on a solution of a dibromocarbene precursor (31 mM) and *tert*-butyl isocyanide (TBI) (0.53 mM) in CH_2Cl_2 and the resulting infrared active adduct was observed at 2040 cm^{-1}. The formation of this ketenimine species enabled the lifetime of dibromocarbene (DBR) in CH_2Cl_2 to be determined by nanosecond time-resolved infrared spectroscopy (τ = 8 ns). The structure of the infrared active species was confirmed by Density Functional Theory calculations (B3LYP/6-31G*) which

predicted the infrared absorbance of the ketenimine adduct formed in the reaction of TBI and the infrared inactive DBR species at 2050 cm^{-1} after scaling by a factor of 0.9614.[1]

The lifetime of singlet dibromocarbene (1.05 mM) in CH_2Cl_2 was subsequently confirmed using laser flash photolysis spectroscopy at the visible wavelength of 482 nm for data verification purposes (τ = 35 ns). The nanosecond time-resolved infrared spectroscopic technique was found to provide a dibromocarbene lifetime in CH_2Cl_2 that was in fair agreement with laser flash photolysis UV-Vis experiments. However, the TRIR experiments were conducted using a dibromocarbene precursor solution five hundred times more concentrated than that of the LFP experiments. Dibromocarbene can react with precursor, thus its lifetime (zero [pyridine]) is expected to be shorter in TRIR than in LFP experiments. In conclusion, the dibromocarbene trapping technique utilizing the infrared activity of its ketenimine adduct was successfully employed, and the experimentally determined dibromocarbene lifetime was independently verified by laser flash photolysis experiments.

ACKNOWLEDGEMENTS

I would like to thank my research advisor, Professor Matthew Platz, for the opportunity to conduct undergraduate research in his laboratory and for guiding and helping me mature as a scientist.

I thank Dr. Eric Tippmann, Dr. Sarah Mandel, Mr. Xiaofeng Shi, and the entire Platz Group for their mentorship, encouragement, and instruction in the laboratory.

I would like to thank Professor Todd Lowary for all his advice and support both inside and outside of the laboratory and classroom. I would never have been able to enjoy such a rewarding and successful undergraduate career without his encouragement and help over the past five years.

I would like to especially thank my family for always striving to help me receive the best education possible and providing me with so much more than I could have ever asked.

VITA

April 21, 1982…….Born - Columbus, Ohio

2000 - present……..Undergraduate Student,
The Ohio State University, Columbus, Ohio

FIELDS OF STUDY

Major Field: Chemistry
Major Field: Physics

TABLE OF CONTENTS

LIST OF TABLES

LIST OF FIGURES

LIST OF FIGURES CONTINUED

CHAPTER 1: INTRODUCTION

A carbene has been defined as "a divalent carbon compound having two, singly covalently bonded substituents and two unshared electrons."[2] These chemical species are of particular interest to chemists because of their ability to add across carbon-carbon double bonds to form cyclopropane rings and to bind to metal ligands. The purpose of this project was to develop a technique for trapping carbenes and nitrenes with a standard reagent that will form an infrared (IR) active product. The development of a versatile IR trapping probe is desirable because it would allow the direct observation of reaction kinetics for carbene or nitrene systems when pyridine ylide LFP trapping procedures are unsuitable. The carbene and nitrene traps studied were *tert*-butyl isocyanide (TBI) Figure 1.1 and 1.2, and butyl disulfide (BSB) Figure 1.3 and Figure 1.4.

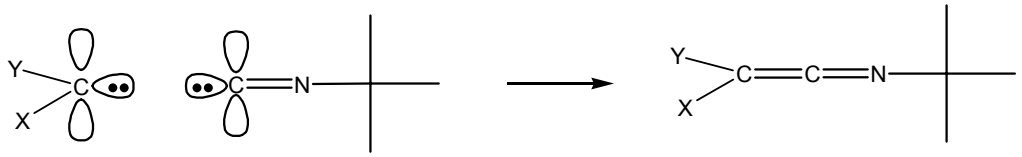

Carbene and Trap IR Active Product

Figure 1.1. *tert*-Butyl isocyanide trapping of a singlet carbene.

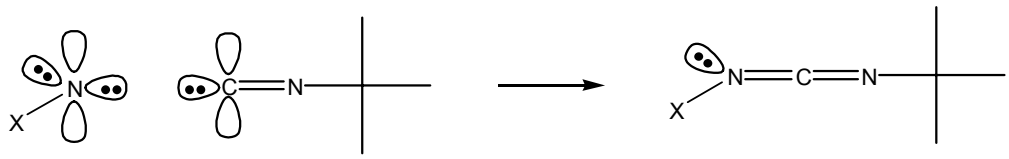

Nitrene and Trap IR Active Product

Figure 1.2. *tert*-Butyl isocyanide trapping of a singlet nitrene.

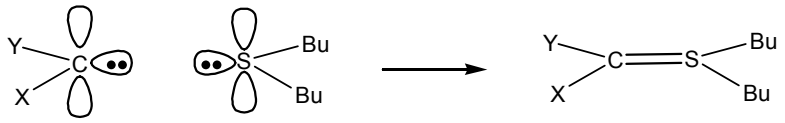

Carbene and Trap IR Active Product

Figure 1.3. Butyl disulfide trapping of a singlet carbene.

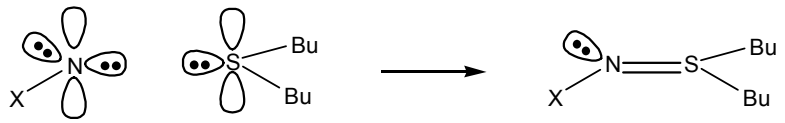

Nitrene and Trap IR Active Product

Figure 1.4. Butyl disulfide trapping of a singlet nitrene.

CHAPTER 2: INVESTIGATION OF POTENTIAL CARBENE AND NITRENE PRECURSORS

2.1. Computational Study of Carbene and Nitrene Candidates for Trapping Studies.

A total of seven carbene and four nitrene candidates were evaluated to determine their suitability for use in the proposed trapping experiments. Both Fourier-Transform Infrared (FTIR) and Ultraviolet-Visible (UV-Vis) spectra of precursors were collected. Infrared absorption of both the reactive intermediate and the expected trapping product from reaction with t-butyl isocyanide and methyl disulfide were calculated for each reactive intermediate using the Gaussian 98 (B3LYP/6-31G* method with a scaling factor of 0.9614)[1] at The Ohio Super-Computing Center (OSC). Calculations of the spectra of the products of the reactive intermediates with butyl disulfide were conducted instead with methyl disulfide to reduce the time needed and the cost of supercomputer use. The UV-Vis absorption of the carbene and nitrene intermediates as well as their expected trapping products were also calculated for each potential precursor using Gaussian 98 (B3LYP/6-31+G**) at the OSC.

2.2. Experimental Collection of FTIR and UV-Vis Spectra for Potential Precursors and Trapping Reagents.

Solid samples (1-2 mg) of the available carbene and nitrene precursors were dissolved in CH_2Cl_2 (0.5 mL). FTIR spectra were then collected of the resulting solutions, neat liquid samples of the remaining precursors, and *n*-butyl isocyanide (Appendix A).

Samples (2-10 mg) of the available potential carbene and nitrene precursor species were dissolved in CH_2Cl_2 (100.0 mL) and UV-Vis spectra were collected of the resulting solutions and a neat liquid sample of *n*-butyl isocyanide (Appendix B). The absorption coefficient (ε) of each sample was then determined at the wavelengths available for the LFP and TRIR laser systems: 266 nm, 308 nm, and 355nm (Tables 2.1- 2.11).

Lambda (nm)	Absorbance	E ($M^{-1}cm^{-1}$)
266	0.88	0.92
308	0.30	0.31
356	0.12	0.12

Table 2.1. Absorption coefficients for neat *n*-butyl isocyanide.

Lambda (nm)	Absorbance	E ($M^{-1}cm^{-1}$)
266	0.61	360
308	0.17	100
356	0.18	110

Table 2.2. Absorption coefficients for chlorophenyl diazirine **A** in CH_2Cl_2.

Lambda (nm)	Absorbance	E ($M^{-1}cm^{-1}$)
266	0.17	700
308	0.068	280
356	0.021	86

Table 2.3. Absorption coefficients for adamantly diazirine **B** in CH_2Cl_2.

Lambda (nm)	Absorbance	E ($M^{-1}cm^{-1}$)
266	1.6	7600
308	2.3	11000
356	0.35	1700

Table 2.4. Absorption coefficients for diazofluorene **C** in CH_2Cl_2.

Lambda (nm)	Absorbance	E ($M^{-1}cm^{-1}$)
266	1.0	6000
308	1.1	6800
356	0.027	160

Table 2.5. Absorption coefficients for diazodibenzocycloheptane **D** in CH_2Cl_2.

Lambda (nm)	Absorbance	E ($M^{-1}cm^{-1}$)
266	1.6	6300
308	1.0	4000
356	0.18	690

Table 2.6. Absorption coefficients for diazoanthrone **E** in CH_2Cl_2.

Lambda (nm)	Absorbance	E ($M^{-1}cm^{-1}$)
266	0.13	1100
308	2.0	17000
356	0.14	1200

Table 2.7. Absorption coefficients for tetrachlorodiazocyclopentadiene **F** in CH_2Cl_2.

Lambda (nm)	Absorbance	E ($M^{-1}cm^{-1}$)
266	0.71	2300
308	0.027	88
356	0.0	0.0

Table 2.8. Absorption coefficients for 2,6-difluorophenyl azide **G** in CH_2Cl_2.

Lambda (nm)	Absorbance	E ($M^{-1}cm^{-1}$)
266	0.15	1300
308	0.089	780
356	0.0	0.0

Table 2.9. Absorption coefficients for 10,10-dibromo[4.3.0]propella-2,4-diene **H** in CH_2Cl_2.

Lambda (nm)	Absorbance	E ($M^{-1}cm^{-1}$)
266	0.91	1900
308	0.034	71
356	0.0	0.0

Table 2.10. Absorption coefficients for benzoyl azide **I** in CH_2Cl_2.

Lambda (nm)	Absorbance	E ($M^{-1}cm^{-1}$)
266	2.90	33
308	3.1	35
356	0.81	9.2

Table 2.11. Absorption coefficients for phenyl azide **J** in CH_2Cl_2.

2.3. Results and Discussion of FTIR, UV-Vis, and Computational Analysis of Potential Precursors and Trapping Reagents.

Experimental and computational results were subsequently evaluated. Trapping products with calculated infrared absorption bands ≥ 50 cm^{-1} from the nearest precursor and trapping reagent peaks were considered acceptable for further investigation. Four of the six carbene precursors and two of the five nitrene precursors studied were determined to be suitable for potential use in trapping experiments by this criterion. Results from the computational investigation of *tert*-butyl isocyanide and methyl disulfide trapping can be found in Table 2.12. As a result of investigating the infrared and ultraviolet-visible characteristics of the potential carbene and nitrene precursors and trapping reagents, dibromocarbene and *tert*-butyl isocyanide were selected as the carbene and trapping reagent to be studied, respectively.

Preliminary investigation of the carbene and nitrene candidates for trapping with *tert*-butyl isocyanide (TBI) indicated that six of the eleven species studied would be suitable for use. Dibromocarbene was selected as the primary species to be studied because of availability of relevant, experimental kinetic data on the carbene species by Platz and Jones, et al.[3]

Precursor	IR Peaks Calculated for t-Butyl Isocyanide Adduct (cm^{-1})	IR Peaks Calculated for Methyl Disulfide Adduct (cm^{-1})
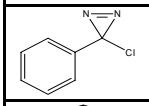 **A**	-	960
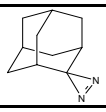 **B**	2045, 1330	-
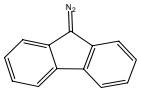 **C**	-	1245, 1110, 960
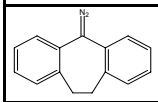 **D**	1345	-
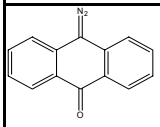 **E**	1365	1195, 1010
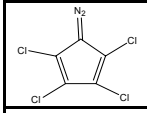 **F**	-	1315, 1230
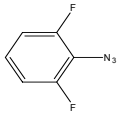 **G**	2160	1270, 990
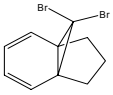 **H**	2050	-
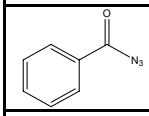 **I**	2175, 1420	1565, 1310, 1305, 1110
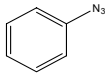 **J**	-	1285
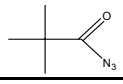 **K**	-	1610, 1260

Table 2.12. Results from computational investigation of infrared activity for products of carbene and nitrene trapping by *tert*-butyl isocyanide and methyl disulfide.

CHAPTER 3: DIBROMOCARBENE

3.1. Computational Results for Dibromocarbene.

Ketenimine **1** formed from the reaction of singlet dibromocarbene (DBR) and *tert*-butyl isocyanide (TBI) was predicted by density functional theory (DFT) calculations (B3LYP/6-31G*) to have a strong infrared absorption band with $\nu \sim 2050$ cm^{-1} (Figure 3.1). This indicated that the product of reaction of dibromocarbene with *tert*-butyl isocyanide should be a suitable system for study by nanosecond time-resolved infrared spectroscopy (TRIR). Similarly, product **3** formed from the reaction of dibromocarbene and butyl disulfide (BSB) was predicted to have a useful infrared absorption, but this reaction has not yet been studied experimentally.

Time-dependent DFT calculations indicated that there is no appreciable UV-Vis absorption of products **1** and **3** above 300 nm. This indicated that the pyridine ylide trapping method would be necessary to determine the rate constant of formation for **1** and **3** by laser flash photolysis (LFP) techniques.

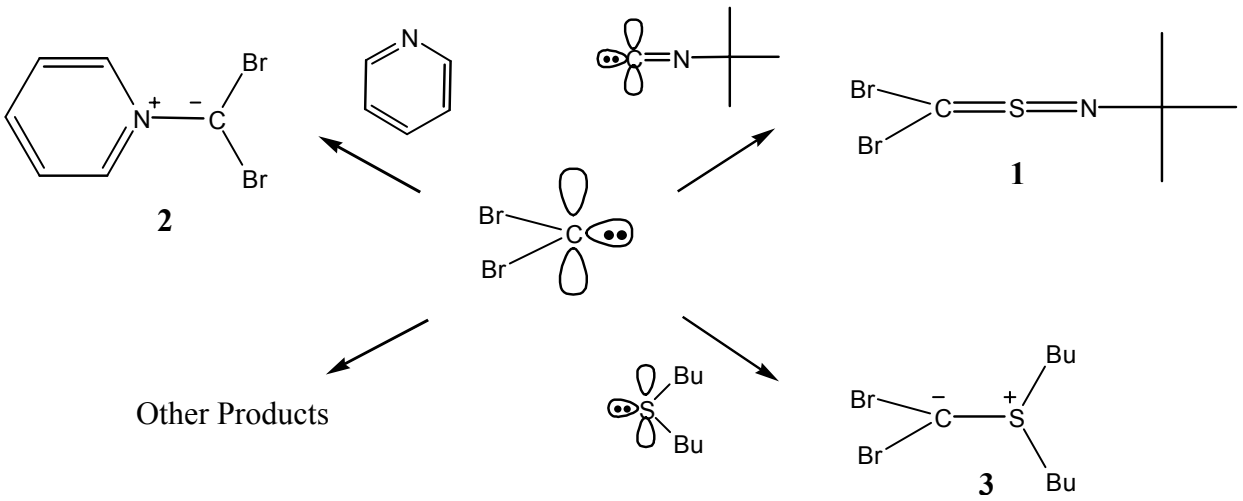

Figure 3.1. Possible reaction of dibromocarbene.

3.2. Laser Flash Photolysis Determination of λ_{max} for the Dibromocarbene Pyridine Ylide.

The dibromocarbene precursor **H**, 10,10-dibromo[4.3.0]propella-2,4-diene, was obtained from Mr. Chris Cassara who synthesized this compound in the Platz Laboratory. A stock solution of 10,10-dibromo[4.3.0]propella-2,4-diene (1.05mM) in CH_2Cl_2 was prepared. A sample solution was made from the stock solution of dibromocarbene precursor **H** and pyridine (5 mM). Singlet dibromocarbene was generated by laser photolysis of the 10,10-dibromo[4.3.0]propella-2,4-diene sample solution with a Lambda Physik LPX-100 excimer laser (XeCl, 308 nm, 20 ns, 50 mJ). Upon LFP, formation of the dibromocarbene pyridine ylide **2** was observed with λ_{max} = 482 nm (Figure 3.2).

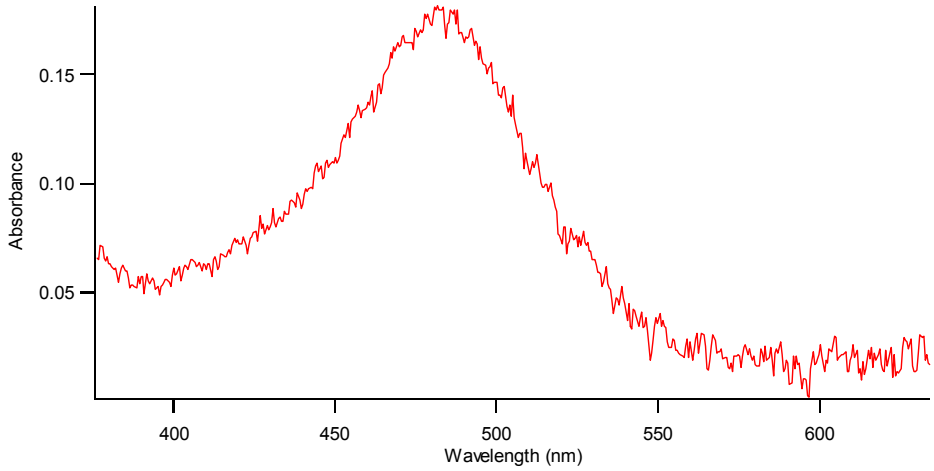

Figure 3.2. Transient spectrum of dibromocarbene pyridine ylide.

3.3. LFP Quenching Study of Dibromocarbene by Pyridine.

The absolute rate constant for the formation of **2** was determined by varying the concentration of pyridine (1-6 mM) in samples of stock solution and performing a kinetic LFP experiment at 482 nm (Figure 3.3). In this experiment the observed pseudo first-order rate constant of carbene formation (k_{obs}) was determined by fitting an exponential to the rising edge of the ylide absorption signals.

The lifetime ($\tau = 1/k_0$) of dibromocarbene in CH_2Cl_2 in the absence of pyridine (Equation 2) and the absolute second-order reaction rate constant of reaction k_{pyr} were determined from a plot of k_{obs} versus [pyridine] (Figure 3.3) and Equation 1. The lifetime of singlet dibromocarbene in CH_2Cl_2 (at this precursor concentration) was determined to be 35 ns in the absence of pyridine and the absolute rate constant of reaction of dibromocarbene with pyridine was determined to have a value of $k_{pyr} = 1.4 \times 10^{10}$ M^{-1} s^{-1}. The lifetime of dibromocarbene in the presence of pyridine (5 mM) in CH_2Cl_2 was subsequently deduced to be 10 ns (Equation 3) under these conditions. The absolute rate constant and lifetime values experimentally determined in this study compare favorably to the reported values of the dibromocarbene-pyridine system in other solvents (Table 3.1).[3]

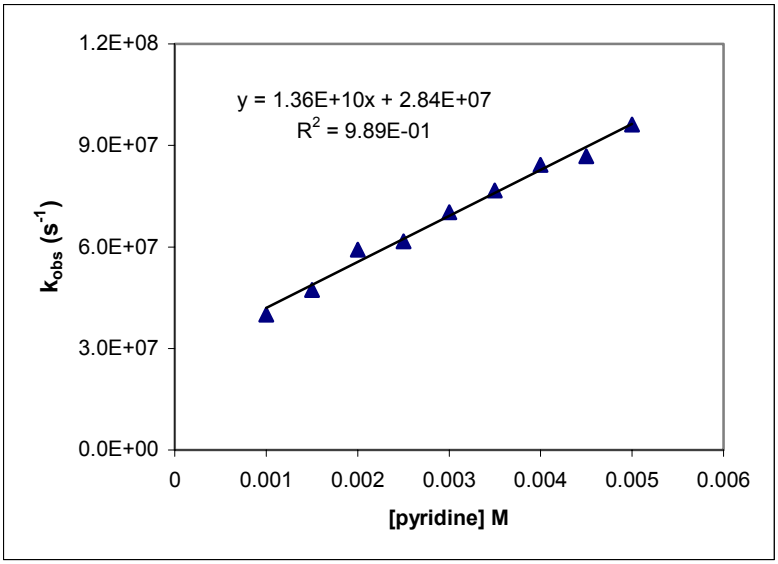

Figure 3.3. A plot of k_{obs} versus [pyridine] at 482 nm and ambient temperature in CH_2Cl_2.

$k_{obs} = k_{pyr}$ [pyridine] + k_0 = k_{pyr} [pyridine] + $1/\tau$ **(Equation 1)**

$= (1.4 \times 10^9\ M^{-1}\ s^{-1})$ [pyridine] + k_0

$k_{pyr} = 1.4 \times 10^9\ M^{-1}\ s^{-1}$ (absolute rate constant of reaction of dibromocarbene with pyridine in CH_2Cl_2)

$\tau = (1/ k_0) = 1/$(y-intercept) **(Equation 2)**

$= (1/(2.8 \times 10^7\ s^{-1}))$

$\tau = 35$ ns (lifetime of singlet dibromocarbene in CH_2Cl_2 in the absence of pyridine and at this precursor concentration)

$1/\tau_1 = k_0 + k_{pyr}$ [pyridine] **(Equation 3)**

$= (2.8 \times 10^7\ s^{-1}) + (1.4 \times 10^{10}\ M^{-1}\ s^{-1})(0.005\ M) = 9.6 \times 10^7\ s^{-1}$

$\tau_1 = 10$ ns (predicted lifetime of singlet dibromocarbene in the presence of pyridine (5 mM) in CH_2Cl_2, from Figure 3.3)

Solvent	Lifetime (ns)	k_{pyr} (10^9 M^{-1} s^{-1})
Dichloromethane	35	14
Isooctane[3]	290	10.8
Freon-113[3]	455 ± 10	4.5
Cyclohexane[3]	350 ± 5	4.95
Cyclohexane-d_{12}[3]	600 ± 30	~5.4

Table 3.1. Lifetimes and quenching rate constants for dibromocarbene by pyridine in a variety of solvents.

3.4. LFP Quenching Study of Dibromocarbene by *tert*-Butyl Isocyanide in the Presence of Pyridine.

Sample solutions were then prepared with dibromocarbene precursor stock solution (1.05 mM in CH_2Cl_2), pyridine (5 mM) and varying concentrations of TBI (0-100 mM). In this experiment the optical yield (A_{482}) of the dibromocarbene pyridine ylide and its observed rate of formation as a function of concentration of t-butyl isocyanide was recorded at λ = 482 nm (Figure 3.4).

A plot of k_{obs} vs [TBI] at constant [pyridine] was constructed (Figure 3.5) and the data was fit to the line: $y = (22.9x + 1.02) \times 10^8$ ($R^2 = 0.964$). The absolute rate constant for ketenimine **1** formation was determined to be $k_{tbi} = 2.3 \times 10^9$ M^{-1} s^{-1} directly from the slope of Figure 3.5 (Equation 4). The lifetime of singlet dibromocarbene in CH_2Cl_2 containing 5 mM pyridine was τ_1 = 30 ns. This is larger than predicted by the data of Figure 3.3. The data from Figure 3.3 is considered to be more accurate than that from Figure 3.5 because TBI reduced the size of the ylide signal thereby reducing the signal to noise ratio.

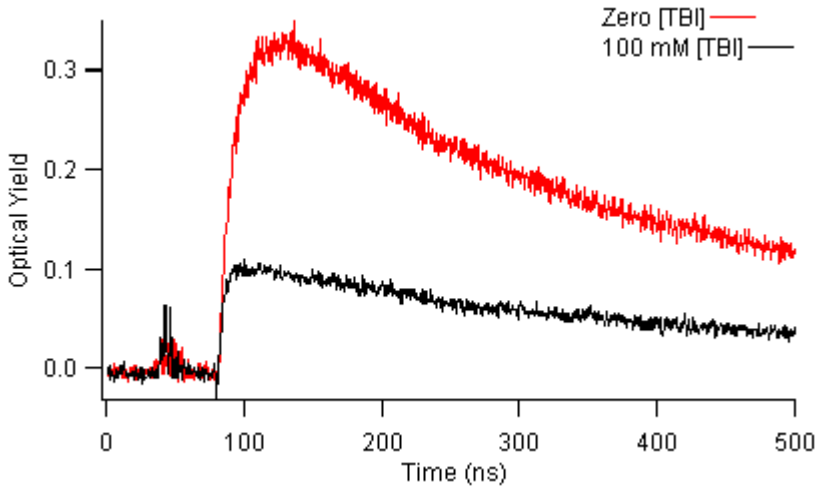

Figure 3.4. Raw LFP data showing quenching of ylide formation with increasing concentration of TBI (0 - 0.1 M) in CH_2Cl_2.

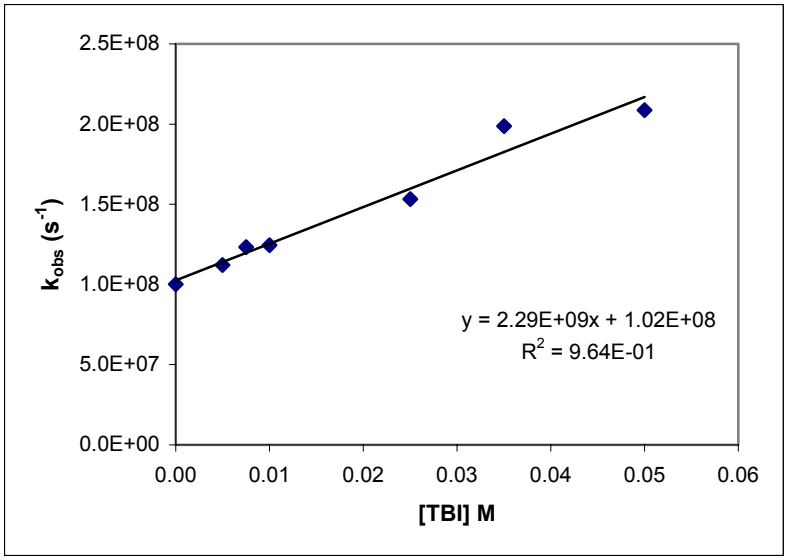

Figure 3.5. k_{obs} versus [TBI] for DBR (1.05 mM) pyridine (5 mM) ylide formation in CH_2Cl_2 at 482 nm.

y-intercept = $(1/\tau_1) + k_{pyr}$ [pyridine] **(Equation 4)**

$1.0 \times 10^8 = (1/\tau_1) + (1.4 \times 10^{10}\ M^{-1}\ s^{-1})\ (0.005\ M)$

$(1/\tau_1) = 3.5 \times 10^7\ s^{-1}$

τ_1 = 30 ns (deduced lifetime of singlet dibromocarbene in the presence of pyridine (5 mM) in CH_2Cl_2, from Figure 3.5)

3.5. Stern-Volmer Data Analysis for LFP Study of Dibromocarbene Quenching by *tert*-Butyl Isocyanide.

The data collected from the LFP quenching study of dibromocarbene by *tert*-butyl isocyanide in the presence of pyridine was analyzed additionally by the Stern-Volmer method (Equation 5).[4] A Stern-Volmer plot of A°_{482}/A_{482} versus [TBI] was constructed (Figure 3.6) and the data was fit to the line: $y = 22.589x + 1.0008$ ($R^2 = 0.991$). Using the previously determined absolute rate constant for ketenimine **1** formation ($k_{tbi} = 2.3 \times 10^9\ M^{-1}\ s^{-1}$, Figure 3.3), the lifetime of dibromocarbene in the presence of pyridine (5 mM) in CH_2Cl_2 was deduced to be 10 ns (Equation 6) in excellent agreement with the data of Figure 3.3.

$$(A^{\circ}_{482}/A_{482}) = 1 + (k_{tbi}[TBI])/(k_{pyr}[pyridine] + 1/\tau) = 1 + k_{tbi}[TBI]\tau_1 \quad \textbf{(Equation 5)}$$

$$\tau = (\text{Stern-Volmer slope}) / k_{tbi} \quad \textbf{(Equation 6)}$$

$$= (22.598\ M) /(2.3 \times 10^9\ M^{-1}\ s^{-1})$$

τ = 10 ns (deduced lifetime of singlet dibromocarbene in the presence of pyridine (5 mM) in CH_2Cl_2, from Figure 3.6)

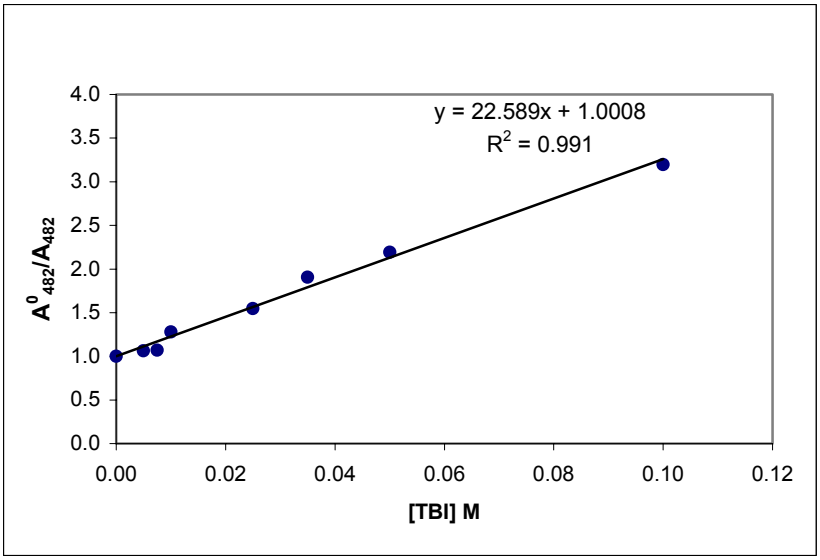

Figure 3.6. Stern-Volmer plot of A°_{482}/A_{482} vs [TBI] for DBR (1.05 mM) ylide formation in CH_2Cl_2 at 482 nm with constant [pyridine] = 5 mM.

3.6. Nanosecond Time-Resolved Infrared (TRIR) Analysis of Dibromocarbene Trapping with TBI.

Calculations predicted a vibrational absorption band of product **1** at $\nu \sim 2050$ cm^{-1}. Thus, a stock solution of 10,10-dibromo[4.3.0]propella-2,4-diene (31 mM) in CH_2Cl_2 was prepared. A sample solution was then prepared containing TBI (0.53 M). A TRIR multi-scan was then performed over the region 2100-2004 cm^{-1} for 9 minutes at DSO 1100 (1100 data points averaged per wavenumber) using a Coherent Infinity XPO/OPO laser (Nd-YAG, 266 nm, 4 ns, 97 Hz repetition rate, 0.4-0.5 mJ/pulse) (Figure 3.7). Signal growth was observed in the region $\nu \sim 2040$ cm^{-1}. A TRIR kinetic scan was then performed at $\nu \sim 2024$ cm^{-1} for 32 seconds and a peak growth was observed with $\tau = 150$ ns (Figure 3.8).

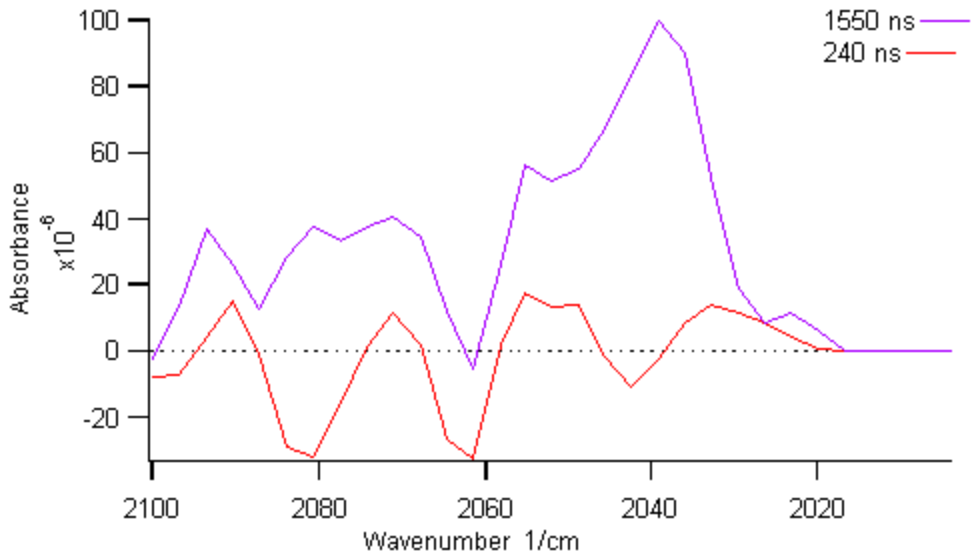

Figure 3.7. TRIR multi-scan of dibromocarbene precursor (31 mM) and TBI (0.53 M) in CH_2Cl_2. DSO 1100.

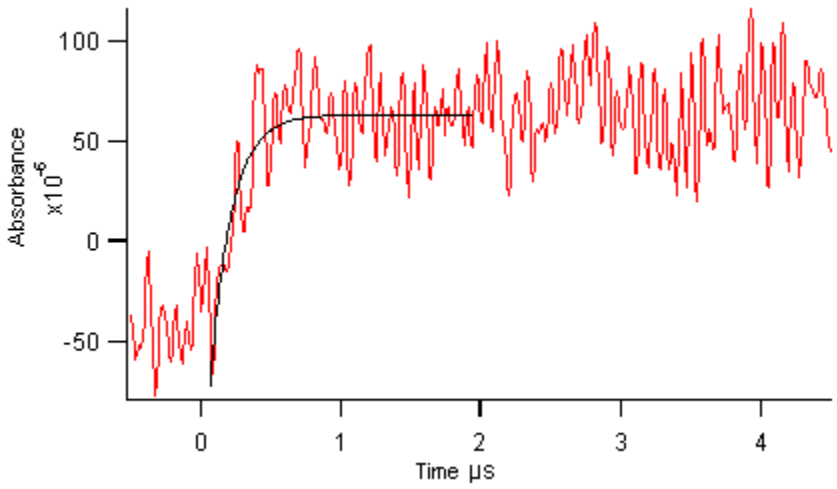

Figure 3.8. TRIR kinetic scan of dibromocarbene precursor (20 mM) and TBI (0.12 M) in CH_2Cl_2. DSO 3000.

Since a value of τ = 150 ns corresponds to a timescale exceeding the time resolution of the TRIR detector, we determined the optical yield (A_k) of ketenimine **1** at varying concentrations of TBI in order to obtain τ from data collected using TRIR techniques. A plot of $1/(A_k)$ vs 1/[TBI] was constructed and fit to the equation y = 392.86x + 7187.9 (R^2 = 0.9932), (Figure 3.9). Using the previously determined value of $k_{tbi} = 2.3 \times 10^9\ M^{-1}\ s^{-1}$ (LFP experiments, Figure 3.3), τ_{TRIR} could be determined from the equation fit to the TRIR data above using Equations 7-9 where Φ_c is the quantum yield of dibromocarbene, Φ_k is quantum yield of ketenimine **1**, and A_k^{∞} is the optical yield of ketenimine **1** at high concentration of TBI.[3] This analysis yields a lifetime of dibromocarbene (τ_{TRIR} = 8 ns) in the absence of pyridine that is in fair agreement with the value determined by LFP with UV-Vis detection (35 ns, Figure 3.3). However, the TRIR experiment used a precursor solution five hundred times more concentrated than that of the LFP experiments. Since dibromocarbene can react with precursor, it is reasonable to expect that the lifetime of DBR (zero [pyridine]) is shorter in TRIR than in LFP experiments.

$$\Phi_k = (\Phi_c\, k_{tbi}\, [TBI]) / (k_0 + k_{tbi}\, [TBI]) \quad \text{and} \quad A_k = \Phi_k\, A_k^{\infty} \qquad \textbf{(Equation 7)}$$

$$1/A_k = (k_0 / \Phi_c\, A_k^{\infty})(1/ k_{tbi}\, [TBI]) + (1 / \Phi_c\, A_k^{\infty}) \qquad \textbf{(Equation 8)}$$

$$(\text{y-intercept} / \text{slope}) = k_{tbi}\, \tau \qquad \textbf{(Equation 9)}$$

$$(7187.9 / 392.86) = (2.3 \times 10^9\ M^{-1}\ s)\, \tau_{TRIR}$$

τ_{TRIR} = 8 ns (lifetime determined of singlet dibromocarbene in CH_2Cl_2 from Figure 3.9)

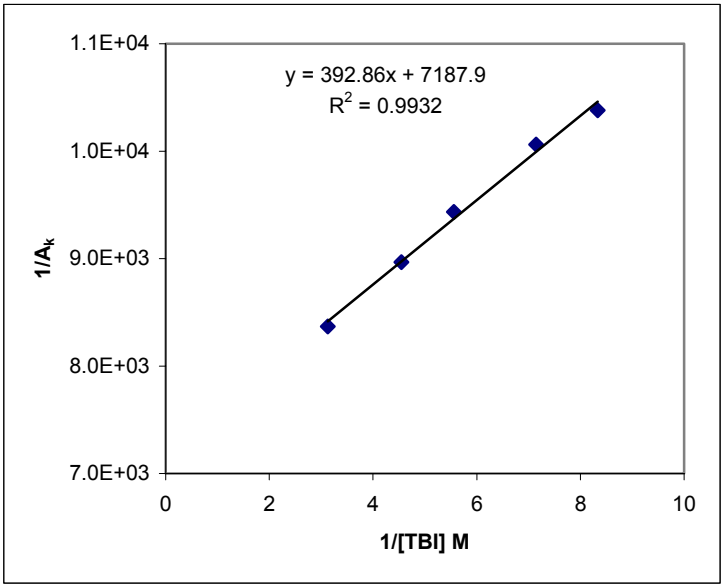

Figure 3.9. TRIR study of optical yield for dibromocarbene precursor (20 mM) and TBI (0.12-0.32 M) in CH_2Cl_2. Timescale 400 ns, DSO 3000.

Using the previously determined value of τ = 35 ns (LFP experiments, Figure 3.3), k_{tbi} can be determined from the equation fit to the TRIR data (Equation 9). This deduced value of $k_{tbi} = 5.2 \times 10^8$ M^{-1} s^{-1} is in fair agreement with the value measured directly in LFP experiments ($k_{tbi} = 2.3 \times 10^9$ M^{-1} s^{-1}, Figure 3.3). However, the 35 ns value of τ used in these calculations is probably too large because of the large precursor concentration used in the TRIR experiment.

(y -intercept / slope) = $k_{tbi}\,\tau$ **(Equation 9)**

(7187.9 / 392.86) = $k_{tbi\ TRIR\ 1}$ (3.52×10^{-8} s^{-1})

$k_{tbi\ TRIR} = 5.2 \times 10^8$ M^{-1} s^{-1}

3.7. Results and Conclusions of Singlet Dibromocarbene Trapping Study.

A technique was developed and employed for the trapping the infrared inactive dibromocarbene species with *tert*-butyl isocyanide resulting in the formation of an infrared active adduct. This dibromocarbene adduct was directly observed by nanosecond TRIR spectroscopy and the lifetime of dibromocarbene τ in CH_2Cl_2 was deduced. The carbene lifetime in dichloromethane was verified by laser flash photolysis experiments and the lifetimes deduced from the TRIR and LFP experiments were in fair agreement supporting the validity and practicality of the carbene trapping/infrared monitoring technique studied.

APPENDIX A

Infrared spectra of carbene and nitrene precursors and *tert*-butyl isocyanide were collected using a Perkin Elmer Spectrum 2000 FT-IR spectrometer.

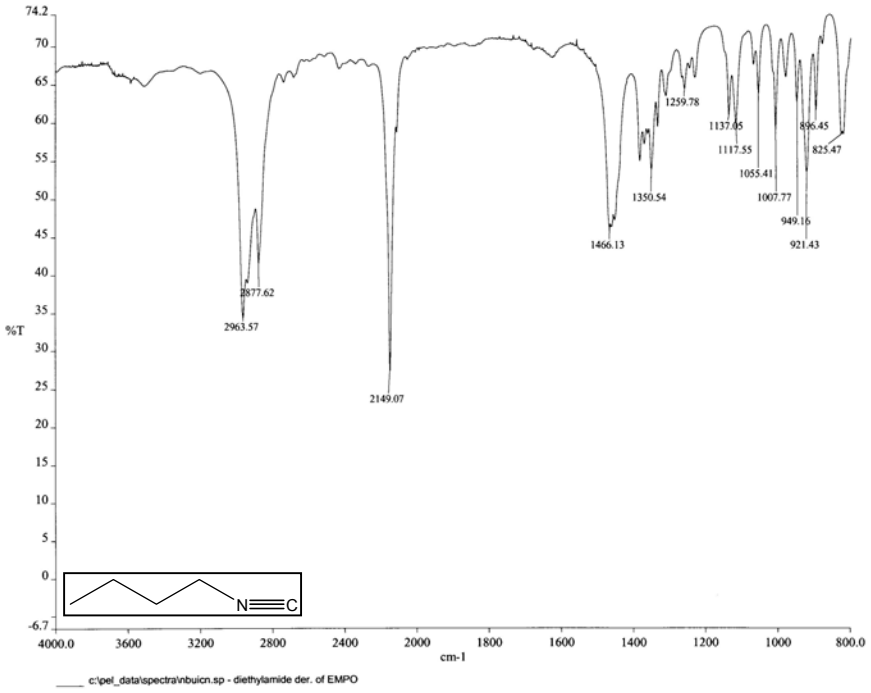

Figure A.1. FTIR spectrum of neat *n*-butyl isocyanide.

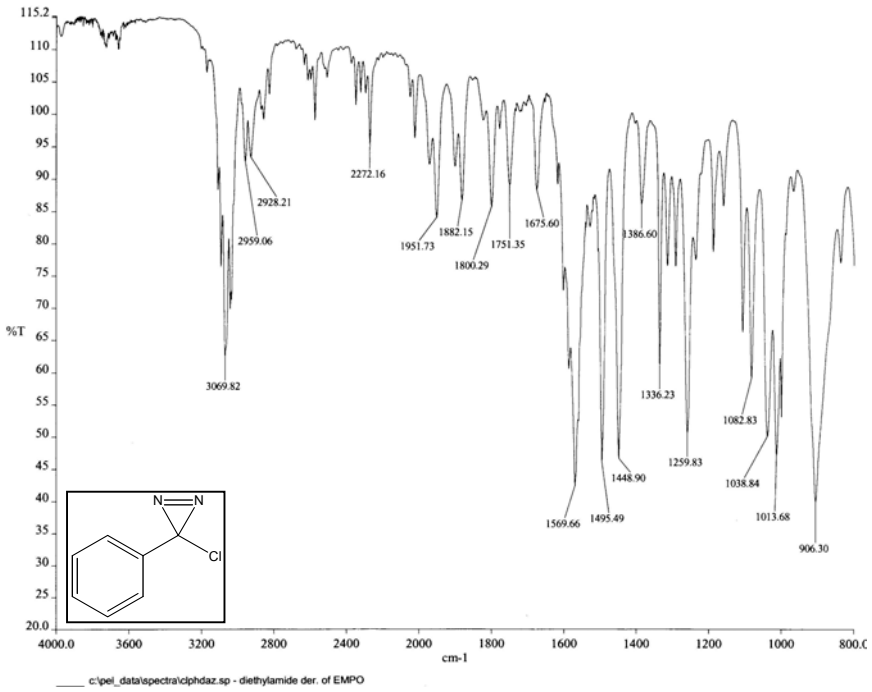

Figure A.2. FTIR spectrum of neat chlorophenyl diazirine **A**.

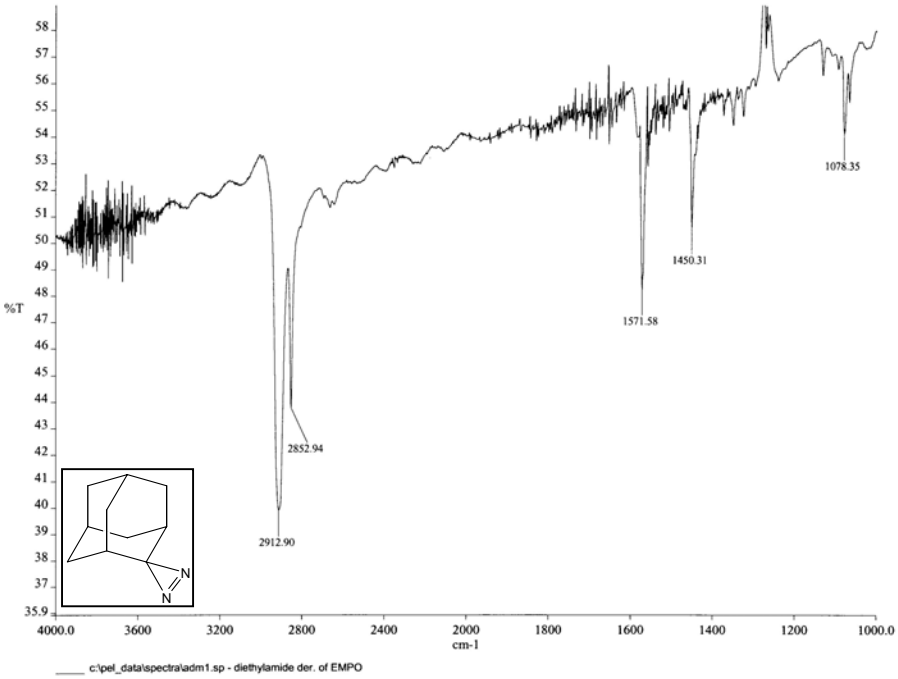

Figure A.3. FTIR spectrum of adamantyl diazirine **B** in CH_2Cl_2.

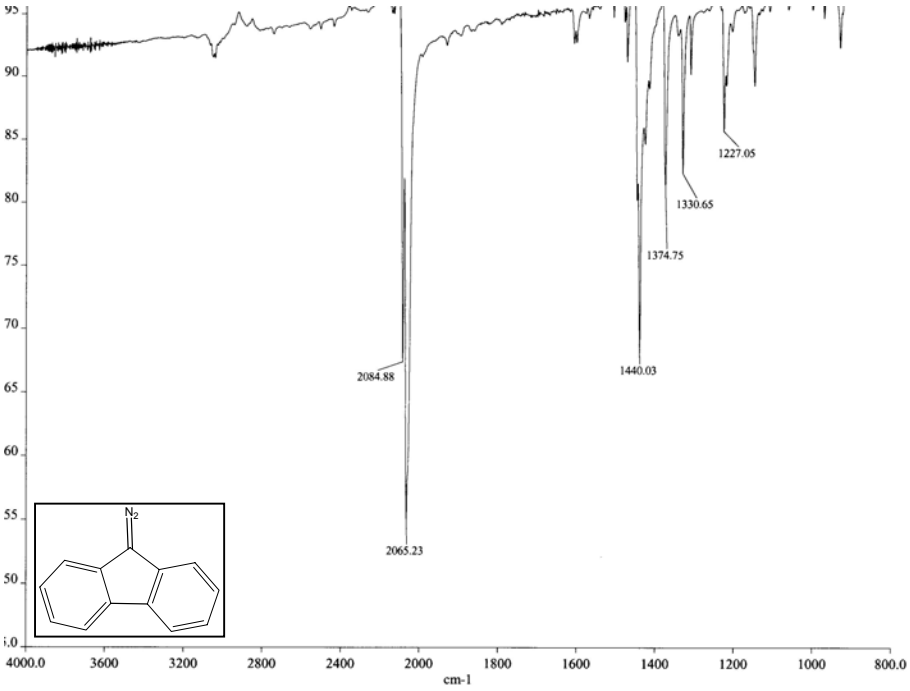

Figure A.4. FTIR spectrum of diazofluorene **C** in CH_2Cl_2.

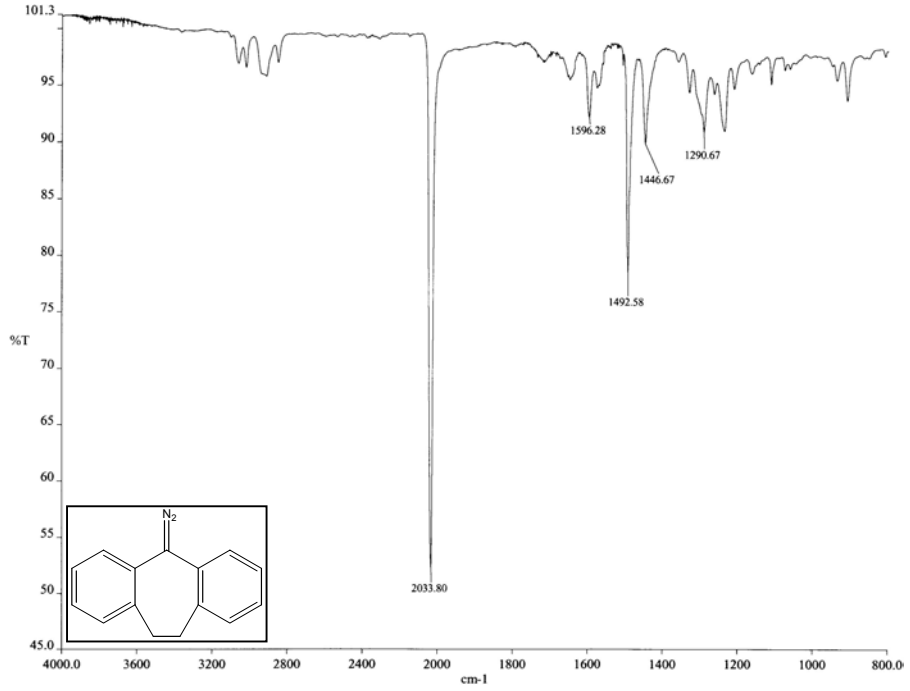

Figure A.5. FTIR spectrum of diazodibenzocycloheptane **D** in CH_2Cl_2.

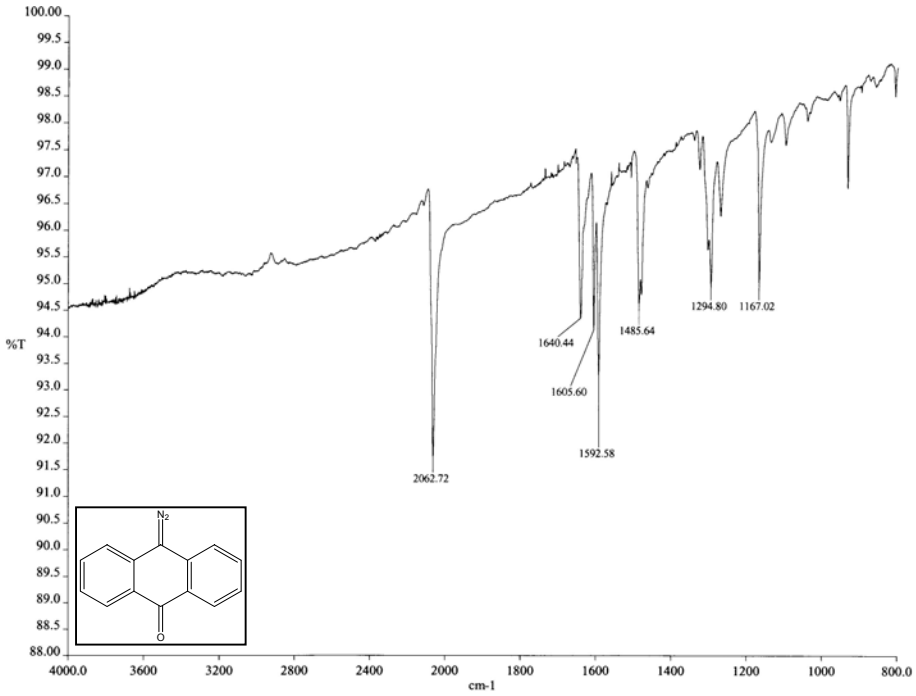

Figure A.6. FTIR spectrum of diazoanthrone **E** in CH_2Cl_2.

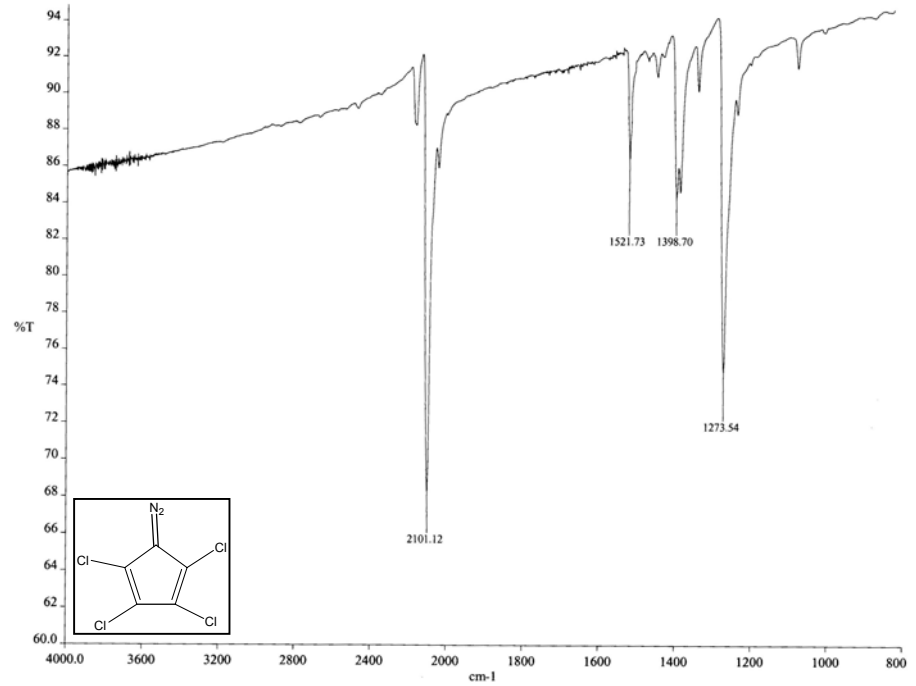

Figure A.7. FTIR spectrum of tetrachlorodiazocyclopentadiene **F** in CH_2Cl_2.

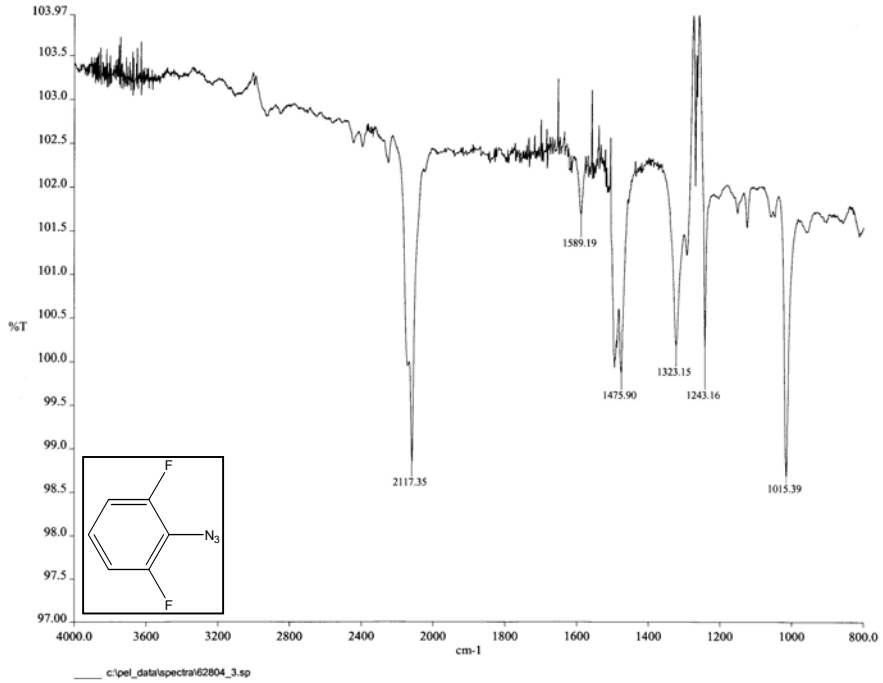

Figure A.8. FTIR spectrum of 2,6-difluorophenyl azide **G** in CH_2Cl_2

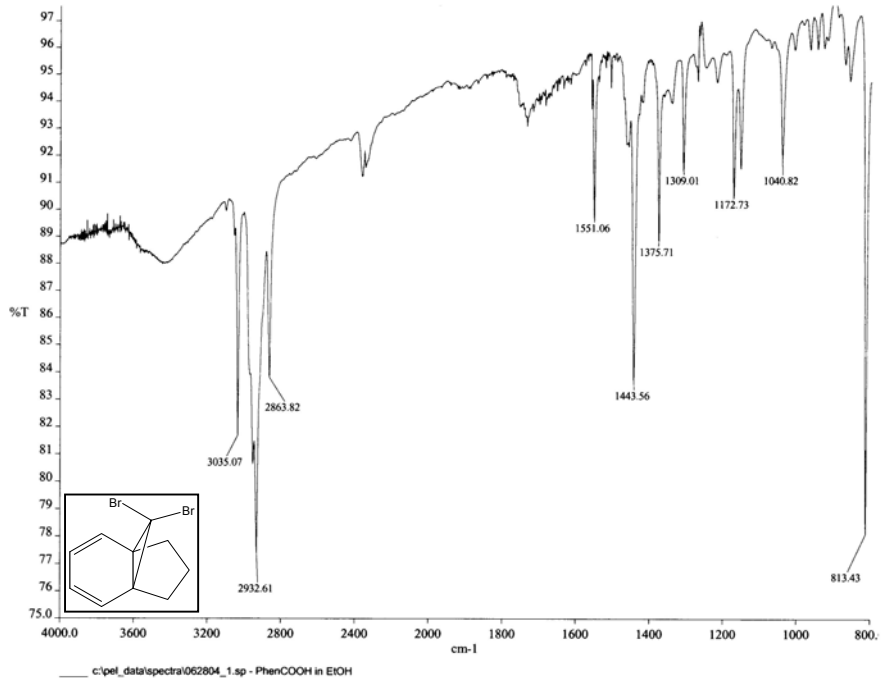

Figure A.9. FTIR spectrum of 10,10-dibromo[4.3.0]propella-2,4-diene **H** in CH_2Cl_2.

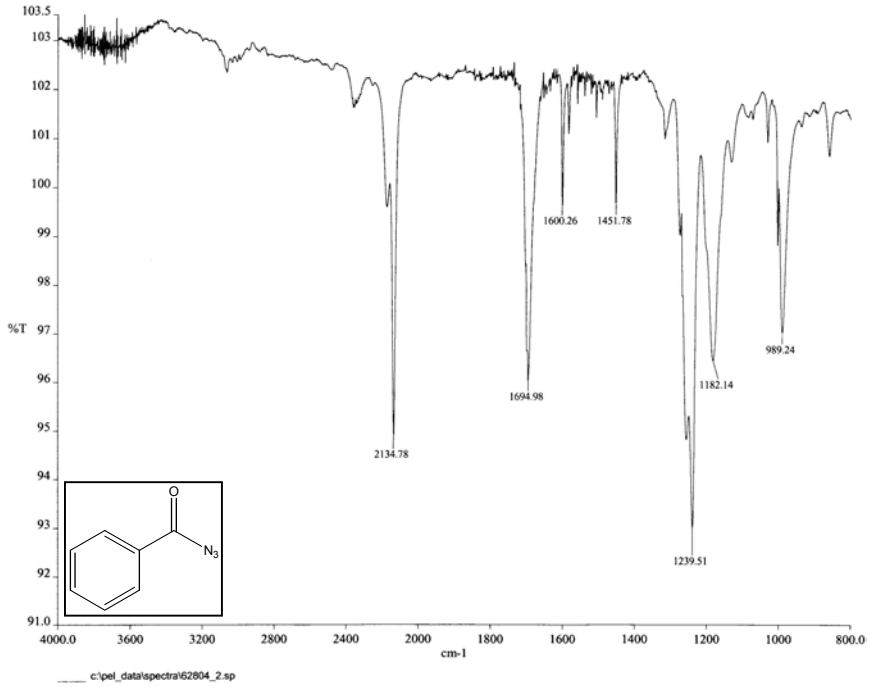

Figure A.10. FTIR spectrum of benzoyl azide **I** in CH_2Cl_2.

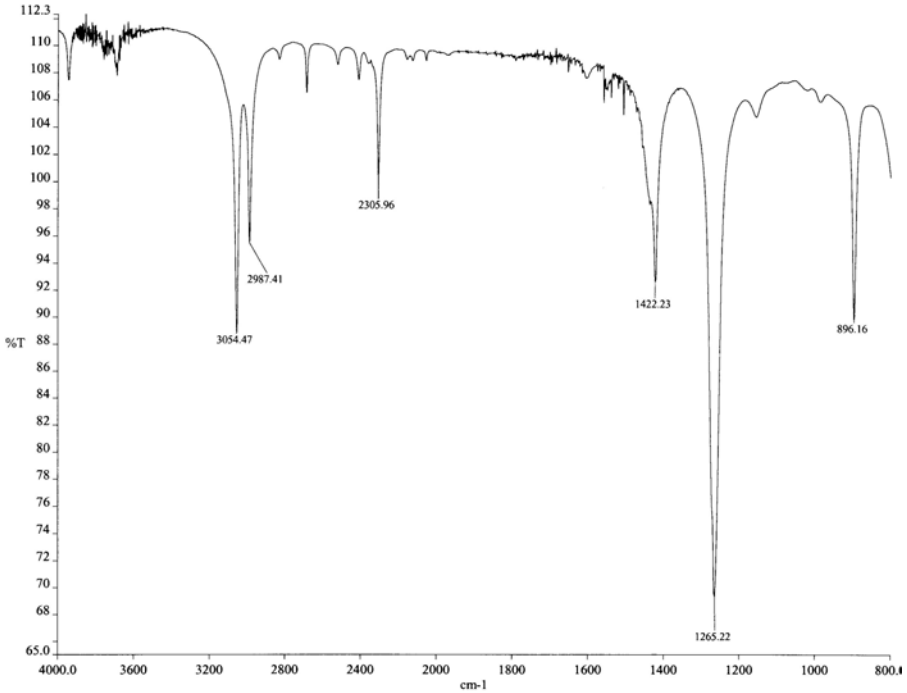

Figure A.11. FTIR spectrum of neat CH_2Cl_2.

APPENDIX B

Ultraviolet-Visible spectra were obtained using a Hewlett Packard 8452 Diode array spectrophotometer.

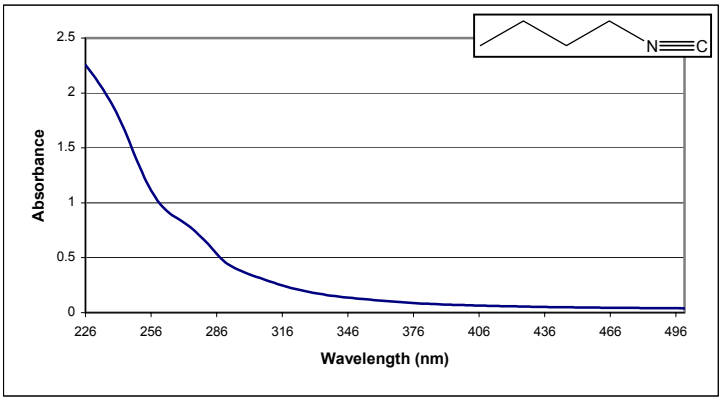

Figure B.1. UV-Vis spectrum of neat *n*-butyl isocyanide.

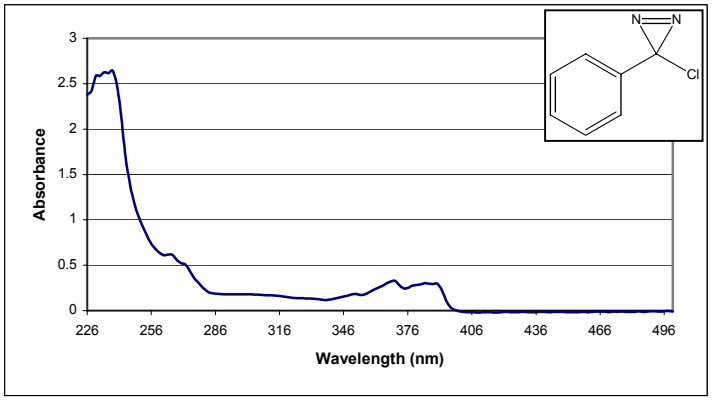

Figure B.2. UV-Vis spectrum of chlorophenyl diazirine **A** in CH_2Cl_2.

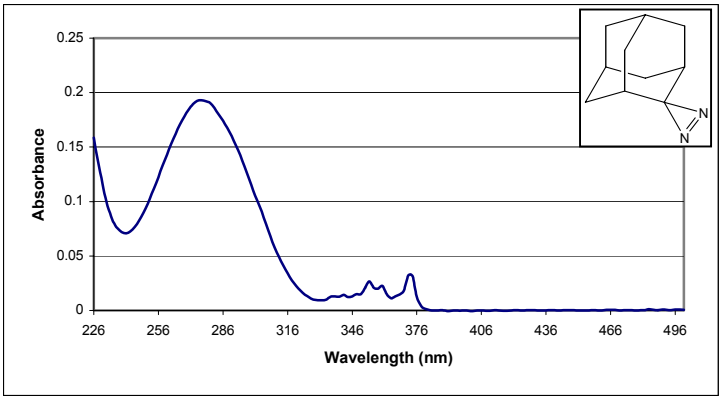

Figure B.3. UV-Vis spectrum of adamantly diazirine **B** in CH_2Cl_2.

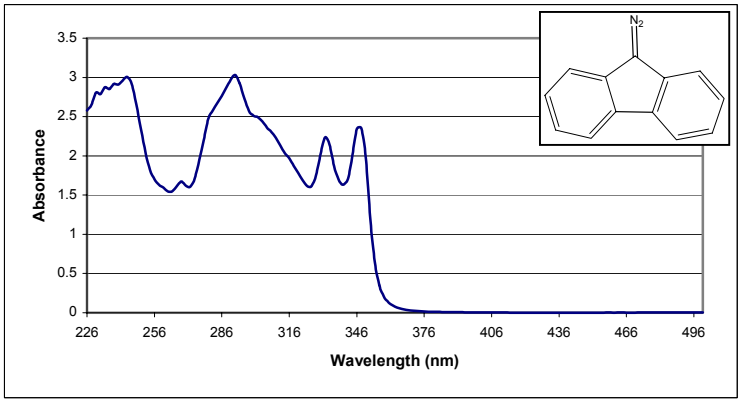

Figure B.4. UV-Vis spectrum of diazofluorene **C** in CH_2Cl_2.

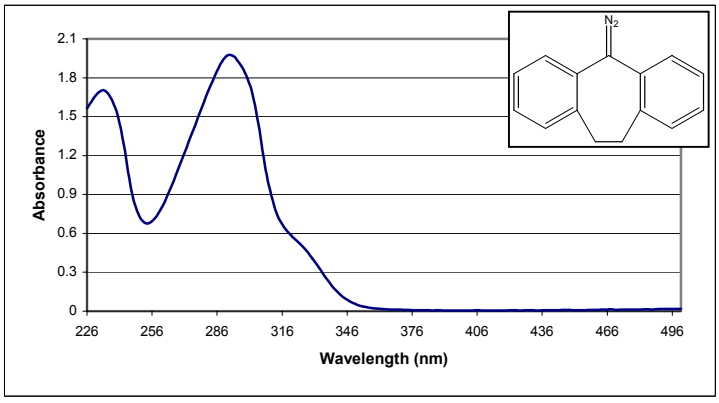

Figure B.5. UV-Vis spectrum of diazodibenzocycloheptane **D** in CH_2Cl_2.

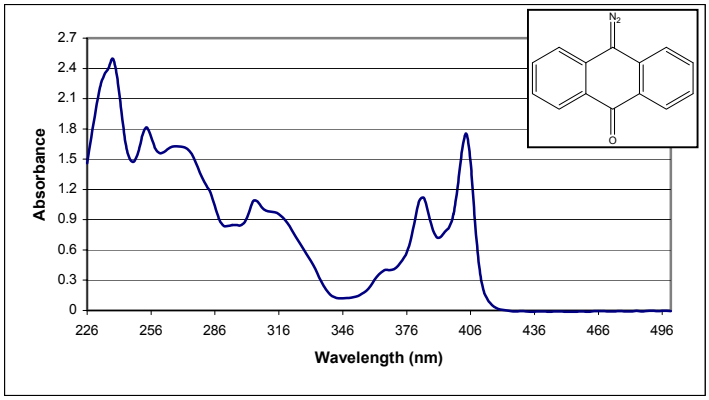

Figure B.6. UV-Vis spectrum of diazoanthrone **E** in CH_2Cl_2.

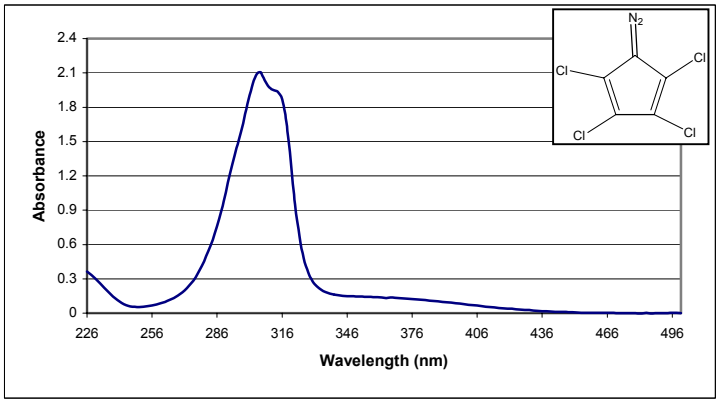

Figure B.7. UV-Vis spectrum of tetrachlorodiazocyclopentadiene **F** in CH_2Cl_2.

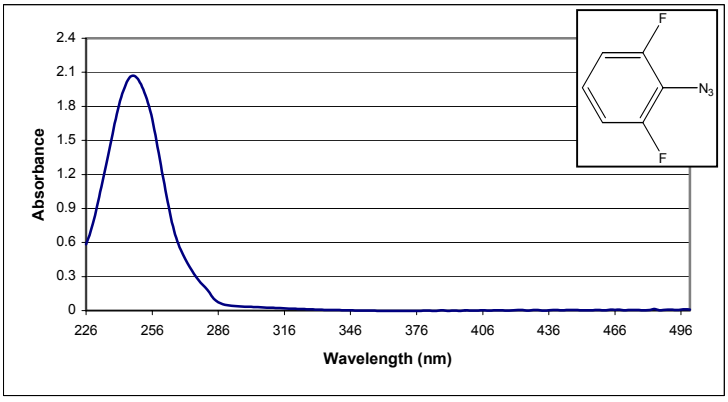

Figure B.8. UV-Vis spectrum of 2,6-difluorophenyl azide **G** in CH_2Cl_2.

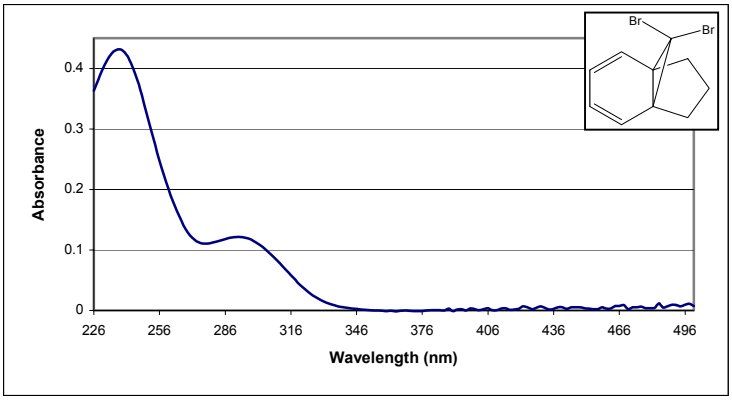

Figure B.9. UV-Vis spectrum of 10,10-dibromo[4.3.0]propella-2,4-diene **H** in CH_2Cl_2.

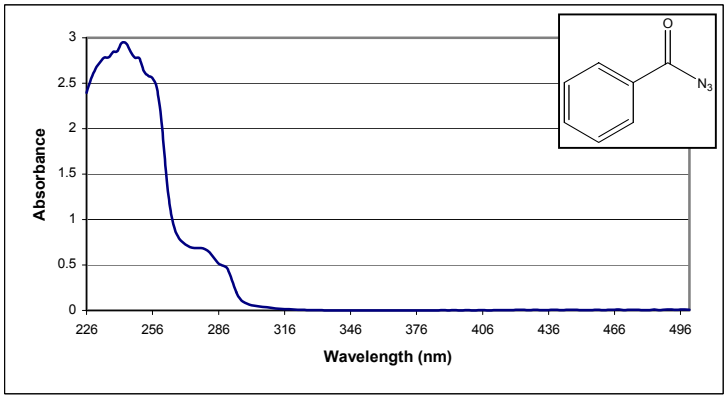

Figure B.10. UV-Vis spectrum of benzoyl azide **I** in CH_2Cl_2.

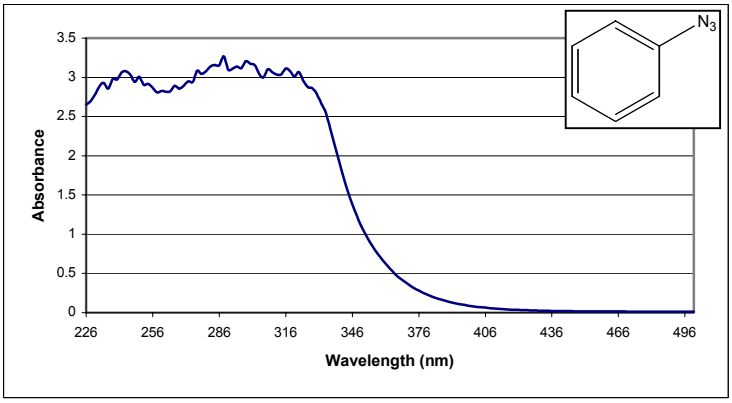

Figure B.11. UV-Vis spectrum of phenyl azide **J** in CH_2Cl_2.

BIBLIOGRAPHY

1. Scott, A. P.; Radom, L. *J. Phys. Chem.*, 1996, 100, 16502.

2. Doering, W. v. E.; Knox, C. H. *J. Am. Chem. Soc.*, 1956, 78, 4947.

3. Robert, M.; Snoonian, J. R.; Platz, M. S.; Wu, G.; Hong, H.; Thamattoor, D. M.; Jones, M. Jr. *J. Phys. Chem. A.*, 1998, 102, 587.

4. Platz, M. S.; Modarelli, D. A.; Morgan, S.; White, W. R.; Mullins, M.; Celebi, S.; Toscano, J. P. *Prog. React. Kin.,* 1994, 19, 93.